



In silico analysis of novel dipeptidyl peptidase-IV inhibitory peptides released from *Macadamia integrifolia* antimicrobial protein 2 (MiAMP2) and the possible pathways involved in diabetes protection

Lei Zhao^{a,*}, Mingxin Zhang^a, Fei Pan^a, Jiayi Li^b, Ran Dou^a, Xinyi Wang^a, Yangyang Wang^a, Yumeng He^a, Shaoxuan Wang^a, Shengbao Cai^{c,**}

^a Beijing Engineering and Technology Research Center of Food Additives, Beijing Technology and Business University, Beijing, 100048, China

^b State Key Laboratory of Microbial Metabolism, Joint International Research Laboratory of Metabolic & Developmental Sciences, School of Life Sciences & Biotechnology, Shanghai Jiao Tong University, Shanghai, 200240, China

^c Faculty of Agriculture and Food, Yunnan Institute of Food Safety, Kunming University of Science and Technology, Kunming, 650500, Yunnan, China

ARTICLE INFO

Handling editor: Dr. Quancai Sun

Keywords:

Macadamia nut protein
Diabetes
Dipeptidyl peptidase IV inhibitors
Molecular docking
Molecular dynamic simulation
Network pharmacology

ABSTRACT

The aim of the present study was to screen novel dipeptidyl peptidase IV (DPP-IV) inhibitory peptides from *Macadamia integrifolia* antimicrobial protein 2 (MiAMP2) and evaluate the potential antidiabetic targets and involved signaling pathways using *in silico* approaches. *In silico* digestion of MiAMP2 with pepsin, trypsin and chymotrypsin was performed with ExPASy PeptideCutter and the generated peptides were subjected to BIOPEP-UWM, iDrug, INNOVAGEN and Autodock Vina for further analyses. Six novel peptides EQVR, EQVK, AESE, EEDNK, EECK, and EVEE were predicted to possess good DPP-IV inhibitory potentials, water solubility, and absorption, distribution, metabolism, excretion, and toxicity properties. Molecular dynamic simulation and molecular docking displayed that AESE was the most potent DPP-IV inhibitory peptide and can bind with the active sites of DPP-IV through hydrogen bonding and van der Waals forces. The potential antidiabetic targets of AESE were retrieved from SwissTargetPrediction and GeneCards databases. Protein-protein interaction analysis identified BIRC2, CASP3, MMP7 and BIRC3 to be the hub targets. Moreover, the KEGG pathway enrichment analysis showed that AESE prevented diabetes through the apoptosis and TNF signaling pathways. These results will provide new insights into utilization of MiAMP2 as functional food ingredients for the prevention and treatment of diabetes.

1. Introduction

Diabetes mellitus (DM) is a metabolic disorder characterized by chronic hyperglycemia, which may cause serious damage to entire body tissues such as the nerves, blood vessels, eyes, kidneys and heart (Bozbulut & Sanlier, 2019). According to the International Diabetes Federation (IDF), 1 in 11 people are living with diabetes around the world and type 2 diabetes mellitus (T2DM) accounts for almost 90% of all diabetes cases (International Diabetes Federation, 2019). Dipeptidyl peptidase IV (DPP-IV) is a key regulator of insulin-stimulating hormones, glucose-dependent insulinotropic polypeptide (GIP) and glucagon-like peptide (GLP-1), thus considered being a promising target for T2DM therapy (Singh et al., 2011). Inhibition of DPP IV leads to enhanced

endogenous GLP-1 and GIP activity, which ultimately improves β -cell function and lowers the blood glucose levels, glucagon secretion and hepatic glucose production (Stemmer et al., 2020). Different DPP-IV inhibitors such as gliptins, sitagliptin and vildagliptin are currently used clinically as T2DM drugs (Patel & Ghate, 2014). However, the frequent use of these drugs can cause side effects. Therefore, it is very important to develop food derived components to increase quality of life for diabetic individuals.

Bioactive peptides have been widely reported to exhibit DPP-IV inhibitory activity (Han et al., 2021). Some of these DPP-IV inhibitory peptides were derived from various foods including milk (Lacroix and Li-Chan, 2014), rice (Hatanaka et al., 2012), salmon (Li-Chan et al., 2012), eggs (Zhao et al., 2020) and meats (Gallego et al., 2014).

* Corresponding author.

** Corresponding author.

E-mail addresses: zhaolei@th.btbu.edu.cn (L. Zhao), caikmust2013@163.com (S. Cai).

<https://doi.org/10.1016/j.crfs.2021.08.008>

Received 8 July 2021; Received in revised form 14 August 2021; Accepted 23 August 2021

Available online 2 September 2021

2665-9271/© 2021 The Authors.

Published by Elsevier B.V. This is an open access article under the CC BY-NC-ND license

(<http://creativecommons.org/licenses/by-nc-nd/4.0/>).

Macadamia integrifolia and *Macadamia tetraphylla* trees are members of the family *Proteaceae* that occurs naturally in subtropical Australia rainforests. In recent years, the planting area of macadamia in China is about 160,000 ha, mainly centered in Yunnan and Guangxi provinces (Tu et al., 2021). Macadamia nuts are popular snack foods, and are rich in fat (~75%) and protein (~8%) (Gwaltney-Brant, 2013). A novel antimicrobial protein (MiAMP2) being a part of 7S globulin was considered to be the most abundant protein in macadamia nuts (Rost et al., 2020). However, to our knowledge, DPP-IV inhibitory peptides identified from MiAMP2 have not been reported.

In silico approaches (e.g., BIOPEP-UWM and ExPASy PeptideCutter) have been successfully applied to predict the release of bioactive peptides from known protein sequences (Pearman et al., 2020). Molecular docking and molecular dynamics (MD) simulation can be further employed to screen and optimize the peptide structures, and predict the interactions between molecules (Zheng et al., 2021). Moreover, network pharmacology has become a powerful tool to reveal the mechanisms underlying the action of bioactive components, as well as identify the potential signaling pathways (Lin et al., 2020). The application of *in silico* and network pharmacology analyses will reduce the time and cost for screening bioactive peptides and disclosing their possible mechanism of action. Therefore, the objectives of this study were to: (i) discover DPP-IV inhibitory peptides from *in silico* digest of MiAMP2 via virtual screening; (ii) investigate the interaction between peptide and DPP-IV using molecular docking and MD simulation; (iii) predict the potential signaling pathways involved in the regulation of diabetes by the most potent DPP-IV inhibitory peptide using network pharmacology analysis.

2. Materials and methods

2.1. *In silico* digestion of MiAMP2

The amino acid sequences of macadamia nut protein MiAMP2 (AMP21, AMP22 and AMP23) were obtained from the UniProtKB database (<https://www.uniprot.org/>) with accession numbers of Q9SPL3, Q9SPL4, and Q9SPL5, respectively. Three representative gastrointestinal proteases of pepsin (EC 3.4.23.1), trypsin (EC 3.4.21.4), and chymotrypsin (EC 3.4.21.1) were chosen for the simulation of proteolysis (Sensoy, 2021). *In silico* digestion of MiAMP2 was carried out using the programs ExPASy PeptideCutter (https://web.expasy.org/peptide_cutter/).

2.2. Virtual screening of DPP-IV inhibitory peptides

The 3D crystal structure of human DPP-IV (PDB ID: 5J3J) was obtained from Protein Data Bank (<https://www.rcsb.org/>), and the unnecessary ligands and water molecules were removed. The peptides with 2–5 amino acids in length generated using ExPASy PeptideCutter were selected for further study. The selected peptides were compared with known DPP-IV inhibitory peptides in BIOPEP-UWM database (<http://www.uwm.edu.pl/biochemia/index.php/en/biopep>) and their amino acid sequences were afterwards converted into Simplified Molecular Input Line Entry Specification (SMILES) strings (Tu et al., 2018). Then, Openbabel 3.1.1 software was applied to convert a number of SMILES strings into 3D molecular structures. The 3D structures of peptides were optimized using the MMFF94 force field (O'Boyle et al., 2011). AutoDock Vina was used to dock peptides and DPP-IV (Trott & Olson, 2010). In brief, the polar hydrogen atoms and Gasteiger charges were added to peptides and DPP-IV using AutoDock Tools software (ADT, version 1.5.6). GetBox plugin (<https://github.com/MengwuXiao/Getbox-PyMOL-Plugin>) was used to design the docking box (x: 18.0, y: 3.2, z: 53.3) in order to cover all amino acid residues in the active sites of DPP-IV (S1, S2 and S3 pockets) (Kim et al., 2018). The semi-flexible docking was performed, and saxagliptin (a DPP-IV inhibitor) was used as positive control.

2.3. ADMET and physicochemical property prediction of DPP-IV inhibitory peptides

According to the results of virtual screening, peptides with affinity greater than or equal to that of saxagliptin were considered as potential DPP-IV inhibitory peptides. *In silico* ADMET properties including absorption, distribution, metabolism, excretion, and toxicity of the selected peptides were estimated by iDrug (<https://drug.ai.tencent.com/cn>), and their physicochemical properties (e.g., isoelectric point and solubility) were computed by INNOVAGEN (<https://pepcalc.com/>).

2.4. Molecular dynamic (MD) simulations

MD simulations were carried out according to our previous methods with slight modifications (Pan et al., 2021). In brief, MD simulations were performed for 50 ns using the GROMACS 19.5 package (<https://manual.gromacs.org/>) with Amber ff99SB-ILDN force field and TIP3P explicit water model for DPP-IV with or without peptides. The AMBER ff99SB-ILDN force field was used to describe the topology and charge of peptides (Lindorff-Larsen et al., 2010). Subsequently, counter ions were added to neutralize the unbalanced charge of the system. Energy minimization (1000.0 kJ/mol/nm) was performed using the steepest descent method. After minimization, the system was subjected to NVT equilibration (0.5 ns, 310.15 K) and NPT equilibration (1.0 ns, 1.0 bar) (Berendsen et al., 1984; Parrinello, & Rahman, 1981). All the systems were simulated by MD for 50 ns. Unless special explanation, all other parameters are consistent with the methods of our previous study (Pan et al., 2021). The GROMACS package (version 19.5) was used to analyze the MD trajectories. The free energy landscape was obtained by means of covariance matrix construction and principal component analysis (PCA) to clearly observe the relationship between Gibbs free energy and structure stability (Chen et al., 2020; Stein et al., 2006). The DPP-IV-peptide complex with the lowest Gibbs free energy was selected for further analysis of interaction between DPP-IV and peptide.

2.5. Screening for potential targets of the selected peptide and diabetes

Potential targets of the selected peptide were evaluated using SwissTargetPrediction (<http://www.swisstargetprediction.ch>) (Daina et al., 2019). The SMILES file of the selected peptide was imported into SwissTargetPrediction website, and the attribute was set to “*Homo sapiens*” for target prediction of the selected peptide. Data on the diabetes-associated gene targets were collected from Genecards database (<https://www.genecards.org/>) with “diabetes” as the key word. Draw Venn Diagram (<http://bioinformatics.psb.ugent.be/webtools/Venn/>) was used to map the potential targets of the selected peptide to the disease targets of diabetes.

2.6. Protein-protein interaction (PPI) network

Search Tool for the Retrieval of Interacting Genes (STRING, <http://string-db.org>) online database was used to construct the PPI network. The organism was set to “*Homo sapiens*”, and the minimum required interaction scores was set to “highest confidence” (> 0.9). The PPI network was then visualized using Cytoscape (Version 3.8.0) and the Molecular Complex Detection (MCODE) plugin was used to find clusters of highly interconnected regions in the PPI network, the parameters were as follows: degree cutoff ≥ 2 , node score cutoff ≥ 0.2 , K-core ≥ 4 , and max depth = 100. Hub genes were screened from the PPI network using the cytoHubba plugin based on 5 topological analysis algorithms (MCC, Degree, BottleNeck, Closeness, and Betweenness) (Chin et al., 2014).

2.7. GO and KEGG pathway enrichment analyses

Metascape (<http://metascape.org/>) is a web-based portal designed

to provide a comprehensive gene list annotation and analysis resource for experimental biologists. It makes use of Gene Ontology (GO) analysis and Kyoto Encyclopedia of Genes and Genomes (KEGG) analysis (Zhou et al., 2019). The targets of anti-diabetes action of the selected peptide were inputted to the Metascape platform with “*Homo sapien*” as the organism and P value cutoff of 0.01. GO annotation analysis and KEGG pathway enrichment analysis on the targets were performed and the results were saved and sorted by the number of targets involved in each entry to screen top biological processes and pathways. Bar graph and bubble chart were plotted by an online platform <http://www.bioinformatics.com.cn>, for analysis and visualization of the GO and KEGG analysis results.

3. Results

3.1. *In silico* digestion of MiAMP2

In silico digestion of MiAMP2 with pepsin, trypsin and chymotrypsin was carried out in our study. As shown in Table S1, a total of 86 peptides composed of 2–5 amino acid residues were released after *in silico* digestion of MiAMP2. The BIOPEP-UWM database has recently become a popular tool for studying bioactive peptides, especially those derived from foods and being constituents of diets that prevent development of chronic diseases. It deposits 4199 bioactive peptide sequences related to different biological functions, of which 421 peptides with 2–5 amino acid residues exhibited DPP-IV inhibitory activities (Minkiewicz et al., 2019). Compared with the DPP-IV inhibitory peptides deposited in BIOPEP-UWM database, QY, NY, EY, DR, EK, VL and VG were previously reported as effective DPP-IV inhibitory peptides (Table S1), indicating the potential of MiAMP2 as a resource for the generation of DPP-IV inhibitory peptides.

3.2. Screening of candidate DPP-IV inhibitory peptides

As an important target for the treatment of T2DM, DPP-IV can degrade incretins including GLP-1 and GIP and cause disorder of blood glucose regulation (Lan et al., 2015). Inhibition of DPP-IV activity leads to increased levels of plasma GLP-1 and insulin, and thereby lowers blood glucose levels. The activity of DPP-IV is closely related to its three active sites, namely S1 (Tyr547, Ser630, Tyr631, Val656, Trp659,

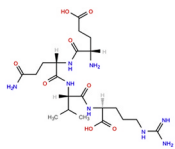
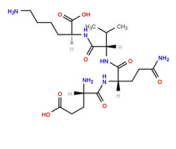
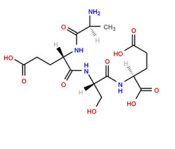
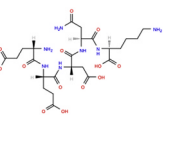
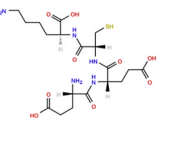
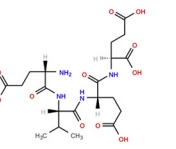
Tyr662, Tyr666, Asn710, Val711 and His740), S2 (Glu205, Glu206, Tyr662) and S3 (Ser209, Arg358 and Phe357) pockets (Pan et al., 2020). Therefore, S1, S2 and S3 pockets were selected as docking targets to screen DPP-IV inhibitory peptides preliminarily. The molecular docking results showed that a total of 53 small peptides had strong DPP-IV binding affinity, which were found to be lower than or equal to that of the positive control saxagliptin (−7.2 kcal/mol) (Table S1). These peptides were comprised of 13 pentapeptides, 22 tetrapeptides, 12 tripeptides and 6 dipeptides, among which four dipeptides QY (−7.9 kcal/mol), NY (−7.7 kcal/mol), EY (−7.7 kcal/mol) and DR (−7.2 kcal/mol) were previously reported as DPP-IV inhibitory peptides (Lan et al., 2015). Notably, the physicochemical properties and absorption of bioactive peptides are also believed to have an important impact on their bioactivities. Therefore, the above 53 candidate DPP-IV inhibitory peptides were conducted for further screening through ADMET and solubility prediction. The computational analysis showed that six peptides including EQVR, EQVK, AESE, EEDNK, EECK, and EVEE were predicted to possess high water solubility and good ADMET characteristics (Table 1), e.g., good Caco-2 permeability ($>10^{-6}$ cm/s) and high human intestinal absorption (HIA) (Probability > 0.5). Moreover, these six peptides were predicted to be non-toxic and have low CYP450 inhibitory probability (< 0.5) (Table 1). Furthermore, molecular docking was conducted to verify the binding between these six peptides and DPP-IV. Fig. 1 shows that all of EQVR, EQVK, AESE, EEDNK, EECK, and EVEE bound into the active sites (S1, S2 and S3 pockets) of DPP-IV, which was consistent with that of saxagliptin, demonstrating that all these candidate peptides can regulate DPP-IV activity through intermolecular interactions.

3.3. Molecular dynamic (MD) simulation study

MD simulation is an effective technique based on Newton’s equation of motion and is commonly used to study the intermolecular interactions at atomic level and the structural dynamic behavior of macromolecules (Chen et al., 2019). In order to investigate the binding stability of these candidate peptides with DPP-IV, MD simulation was carried out for further study. The results are shown in Fig. 2. Root mean square deviation (RMSD) is used to measure the difference in conformation for each frame in a MD trajectory with a reference structure (Pan et al., 2020). Fig. 2A shows the changes in RMSD values of DPP-IV backbone in the

Table 1

Predicted key ADMET parameters for six peptides selected from *in silico* digestion of *Macadamia integrifolia* antimicrobial protein 2 (MiAMP2).

Peptide	EQVR	EQVK	AESE	EEDNK	EECK	EVEE
Structural formula						
Chemical formula	C ₂₁ H ₃₈ N ₈ O ₈	C ₂₁ H ₃₈ N ₆ O ₈	C ₁₆ H ₂₆ N ₄ O ₁₀	C ₂₄ H ₃₉ N ₇ O ₁₃	C ₁₉ H ₃₃ N ₅ O ₉ S	C ₂₀ H ₃₂ N ₄ O ₁₁
Molecular weight	530.58	502.57	434.40	633.61	507.57	504.49
PI	6.86	6.85	0.85	3.69	4.15	0.76
Water solubility	Good	Good	Good	Good	Good	Good
Ames toxicity probability	0.054	0.037	0.034	0.045	0.431	0.035
Hek293 toxicity probability	0.024	0.025	0.018	0.021	0.03	0.021
Hepatic toxicity probability	0.376	0.413	0.419	0.437	0.465	0.431
Caco-2 permeability	1.816	1.394	1.170	1.370	1.448	2.228
HIA probability	0.994	0.993	0.982	0.515	0.915	0.994
CYP1A2	0.300	0.314	0.205	0.213	0.419	0.208
CYP2C19	0.338	0.338	0.268	0.168	0.493	0.169
CYP2C9	0.271	0.294	0.144	0.113	0.448	0.094
CYP2D6	0.341	0.216	0.173	0.098	0.319	0.104
CYP3A4	0.185	0.184	0.08	0.115	0.194	0.112
Affinity (kcal/mol)	−8	−7.6	−7.5	−7.4	−7.3	−7.2

ADMET, absorption, distribution, metabolism, elimination and toxicity.

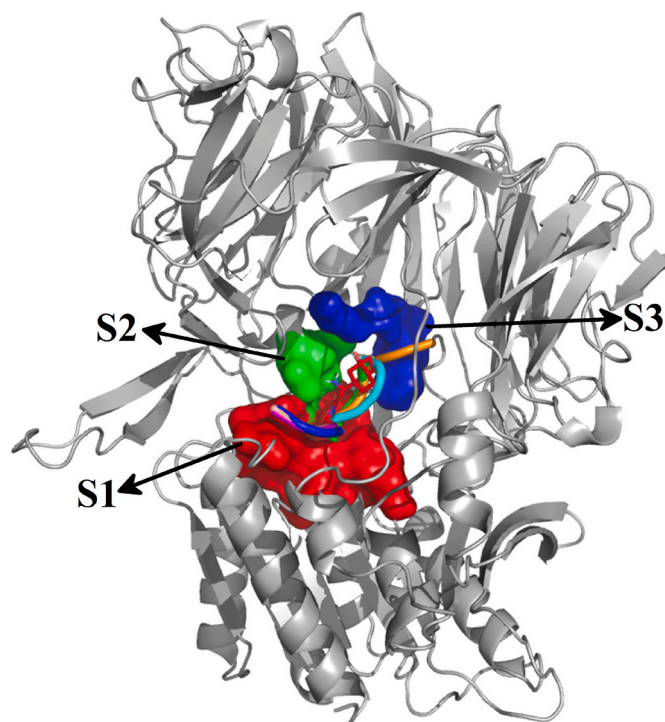


Fig. 1. Molecular docking results of dipeptidyl peptidase IV (DPP-IV) with six peptides selected from *in silico* digestion of *Macadamia integrifolia* antimicrobial protein 2 (MiAMP2).

absence and presence of peptides during the 50 ns MD simulation. For the binary complexes DPP-IV-EQVR and DPP-IV-EECK, the RMSD values of DPP-IV backbone fluctuated greatly within first 25 ns of MD simulation and then reached equilibrium (25–50 ns). By contrast, after binding with AESE, EQVK, EVEE or EEDNK, the RMSD values of DPP-IV backbone kept stable at values lower than 0.25 nm, indicating that DPP-IV backbone remained stable during the whole MD simulation. In order to better study the binding stability of these peptides in the active sites during the 50 ns MD simulation, their RMSD values were also evaluated. As shown in Fig. 2B, AESE showed the best stability of all six candidate peptides with its RMSD value fluctuated gently around a low level (< 0.2 nm) throughout the 50 ns MD simulation, which was helpful for the stabilization of DPP-IV-AESE complex. However, the RMSD values of the other five peptides (EECK, EQVK, EQVR, EVEE and EEDNK) showed drastic fluctuations, indicating that the bindings of these peptides and DPP-IV active sites were not stable enough. Additionally, the results of solvent accessible surface area (SASA) and radius of gyration (Rg) demonstrated that the bindings of these six peptides to DPP-IV had no influence on structure compactness of DPP-IV (Fig. 2C and D).

Root mean square fluctuation (RMSF) reveals the fluctuation of certain residues during simulation process around its average position, which can be used to assess the dynamics stability of system (Ni et al., 2020). Fig. 2E represents the RMSF values of DPP-IV before and after binding with AESE during the 50 ns MD simulation. After binding with AESE, the fluctuations of most key amino acid residues in the active sites of DPP-IV increased obviously. Compared with the initial structure of DPP-IV, higher fluctuations were observed in the active residues of S1 pocket including Phe357, Arg358, Ser630, Tyr631, Val656, Trp659, Tyr662, Tyr666, Asn710, Val711 and His740. Our results suggested that the N-terminal amino acid (Ala) of AESE had strong hydrophobicity, which may play an important role in the binding of AESE and the active sites of DPP-IV.

3.4. Interaction between AESE and DPP-IV

In order to further clarify the interaction between AESE and DPP-IV, the covariance matrix was established using the C α coordinates from MD trajectory of DPP-IV-AESE to calculate the eigenvalues and eigenvectors. The trajectories were projected onto the first two eigenvectors to construct the free energy landscape (Chen et al., 2020). From the free energy landscape (Fig. 3A), two stable binding structures (energy basins) can be extracted. As shown in Fig. 3B, there was no significant difference between these two structures of DPP-IV-AESE and the RMSD value between these two structures calculated by PyMOL was 0.132 nm. This result was consistent with that of MD simulation (Fig. 2) and further proved the good stability of DPP-IV-AESE complex. Fig. 3C and D shows 2D interaction diagram of AESE and DPP-IV in the complex with the lowest Gibbs free energy. AESE formed van der Waals forces with the active residues Tyr547, Ser630, Tyr666 and Phe357 in S1 pocket, while formed a hydrogen bond and a van der Waals force with Glu205 and Glu206 in S2 pocket, respectively. Additionally, the carboxyl groups of glutamic acid residues in AESE interacted with Arg125 and Arg560 of DPP-IV through salt bridges (Fig. 3C). Hydrophobic interactions were also found between AESE and aromatic amino acid residues Phe357 (S2 pocket), Tyr547 and Tyr666 (S1 pocket) in DPP-IV (Fig. 3D), which was consistent with the RMSF analysis, suggesting that hydrophobic interactions in the S1 pocket are crucial for DPP-IV inhibitory peptides and the interaction at the S2 pocket may improve affinity (Araki et al., 2020; Nongonierma et al., 2014). Based on these computational methods, tetrapeptide AESE was thought to have the possibility to become an effective inhibitor for DPP-IV.

3.5. Potential targets of AESE against diabetes and PPI network analysis

Target prediction of AESE was carried out using SwissTargetPrediction and a total of 100 putative targets were identified. After sorting from GeneCards database, 14950 diabetes-related targets were obtained. Then, the 100 putative targets of AESE were mapped to 14950 diabetes-related targets using Draw Venn diagram, and 82 intersection targets were filtered as the potential targets of AESE in the treatment of diabetes (Fig. 4A).

PPI network plays a vital role to widely understand molecular function activities. The 82 intersection targets obtained above were further analyzed using the STRING database to construct a PPI network, which contains 58 nodes (without disconnected node) and 115 edges (Fig. 4B). Our results showed that the average number of neighbors (average neighborhood connectivity) was 4.75, and 33 target genes had higher neighborhood connectivity than the average level. Further cluster analysis of the complex network was done using the MCODE plugin in Cytoscape software to generate the highly connected sub-network (Fig. 4C). The results showed that 4 significant clusters were selected from PPI network. The scores of these 4 clusters were 7, 5, 4 and 4, respectively. Cluster 1 had 7 nodes with 21 edges; Cluster 2 had 5 nodes with 10 edges; and both Cluster 3 and Cluster 4 owned 4 nodes with 6 edges. These sub-networks focused on genes involved in IL-17 signaling pathway, relaxin signaling pathway, neuroactive ligand-receptor interaction, proteasome, apoptosis, and apoptosis-multiple species pathways. According to their scores calculated using five topological algorithms (MCC, Degree, BottleNeck, Closeness, and Betweenness), the genes were ranked and the top 10 genes were filtered as hub genes (Table 2). A Venn diagram was constructed to identify common hub genes (Fig. 4D). BIRC2 and CASP3 were overlapped according to five algorithms, and MMP7 and BIRC3 were overlapped according to four algorithms.

3.6. GO analysis and KEGG enrichment analysis of target genes

To further explore the various mechanisms of the protective action of AESE against diabetes, GO annotation and KEGG enrichment analyses of the 82 predicted targets were performed using the Metascape database.

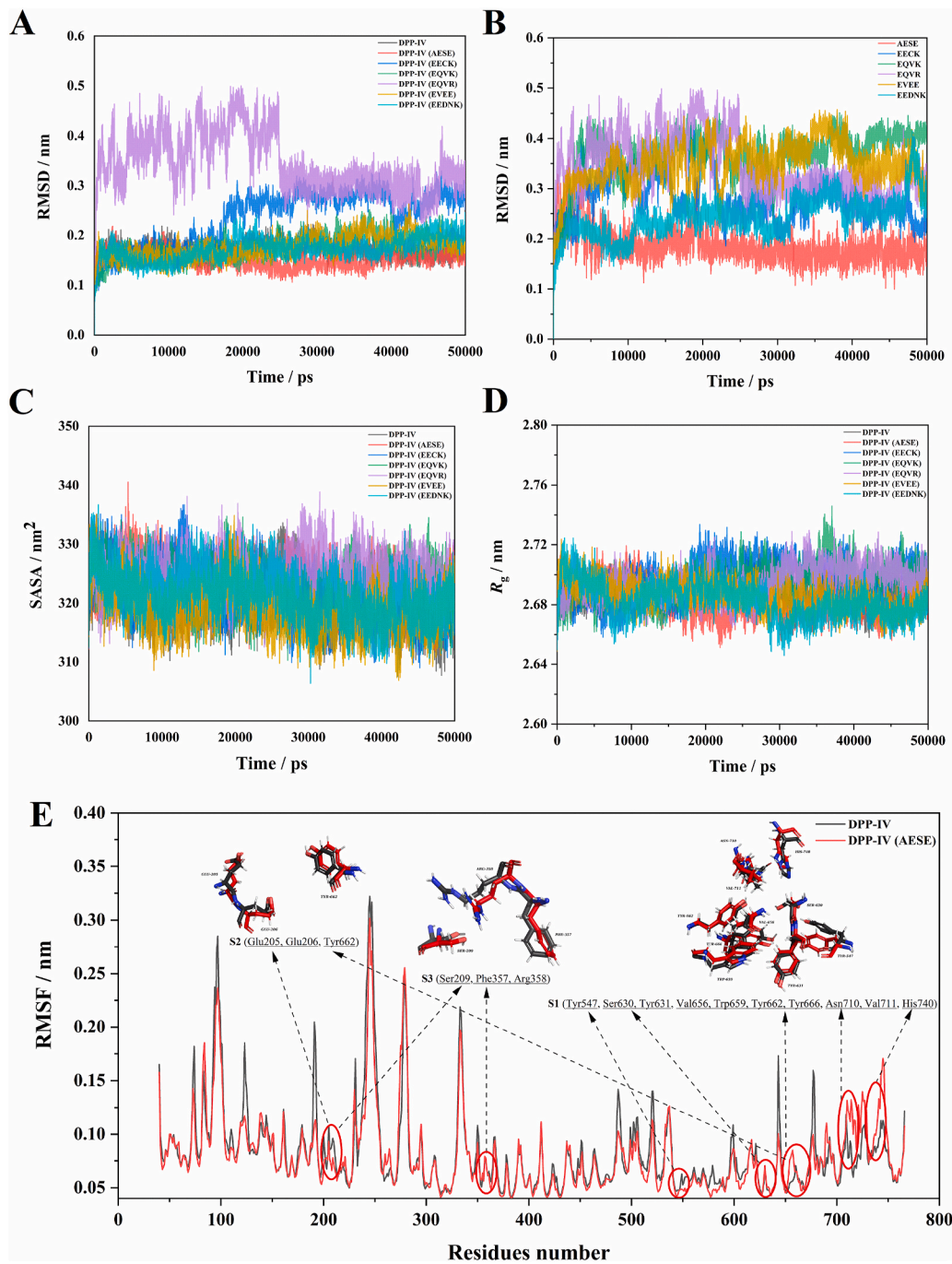


Fig. 2. Molecular dynamics (MD) simulation of dipeptidyl peptidase IV (DPP-IV) in the presence or absence of six candidate peptides. (A) Root mean square deviation (RMSD) of DPP-IV backbone; (B) RMSD of six candidate peptides; (C) Solvent accessible surface area (SASA) of DPP-IV; (D) Radius of gyration (R_g) of DPP-IV; (E) Root mean square fluctuation (RMSF) of DPP-IV.

The threshold value $P < 0.01$ was set to screen out the front GO annotation results and KEGG pathway. GO analysis was typically focused on three aspects: biological process (BP), molecular function (MF) and cell composition (CC). The top 10 enriched BP, MF and CC terms are shown in Fig. 5A. The BP results suggested that these targets participated in collagen catabolic process, positive regulation of defense response, peptide hormone processing, cellular response to abiotic stimulus, histone H3 deacetylation, etc. The CC results indicated that these targets were mainly involved in extracellular matrix, membrane raft, transcriptional repressor complex, lytic vacuole, proteasome core complex, etc. For MF, these targets were mainly associated with endopeptidase activity, metallopeptidase activity, aspartic-type endopeptidase activity,

NAD-dependent histone deacetylase activity, exopeptidase activity, etc. Furthermore, the KEGG enrichment analysis demonstrated that these targets were significantly enriched in multiple pathways including apoptosis, TNF signaling pathway, Alzheimer disease, renin-angiotensin system, and transcriptional misregulation in cancer (Fig. 5B). Above all, the apoptosis pathway was found to be the most enriched pathway, and AESE against diabetes by acting on multiple targets which participate in various processes in this pathway.

4. Discussion

Currently, numerous of natural and synthetic peptides were found to

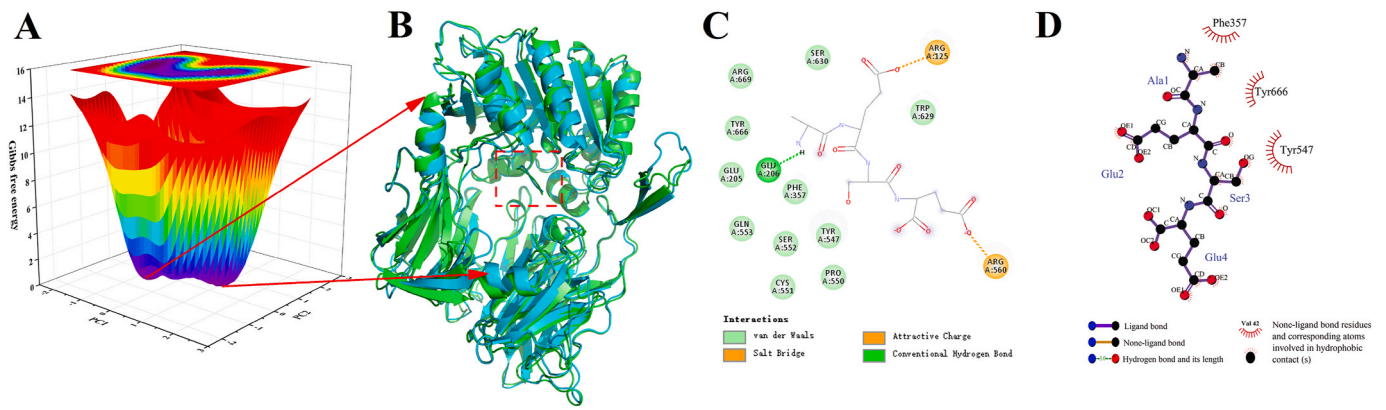


Fig. 3. The binding free energy landscapes and interactions of dipeptidyl peptidase IV (DPP-IV) with AESE. (A) Free energy landscapes of DPP-IV-AESE; (B) The lowest energy conformation of DPP-IV-AESE; (C) 2D Interactions of DPP-IV and AESE.

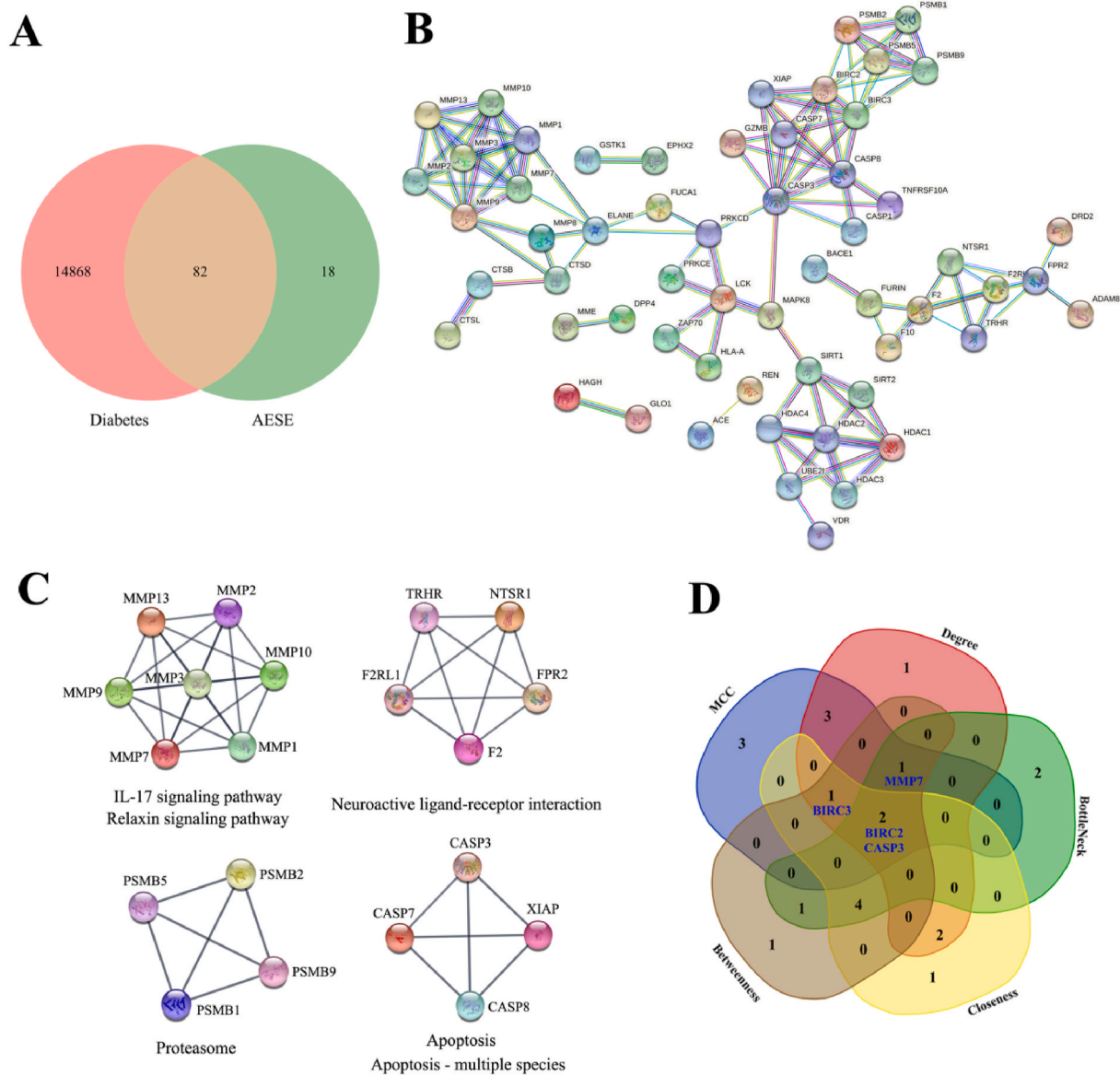


Fig. 4. Protein-protein interaction (PPI) network analysis and hub gene selection (A) Venn diagram of AESE and diabetes targets; (B) PPI network with 58 nodes and 115 edges; (C) Four Clusters with scores of 7, 5, 4 and 4, respectively; (D) Venn diagram of gene sets ranking top 10 based on five topological analysis algorithms in cytoHubba plugin.

Table 2

Top 10 hub genes ranked in cytoHubba for the potential targets of AESE against diabetes.

Catalog	Rank methods in cytoHubba				
	MCC	Degree	BottleNeck	Closeness	Betweenness
Gene symbol top 10	MMP7	CASP3	CASP3	CASP3	CASP3
	MMP9	BIRC3	ELANE	PRKCD	PRKCD
	MMP1	BIRC2	PRKCD	BIRC3	ELANE
	MMP13	CASP8	MAPK8	BIRC2	MAPK8
	MMP3	MMP9	F2	CASP8	SIRT1
	MMP10	MMP7	SIRT1	ELANE	LCK
	MMP2	MMP1	MMP7	MAPK8	CTSD
	BIRC3	FPR2	LCK	CASP7	BIRC3
	BIRC2	MMP13	HDAC2	LCK	BIRC2
	CASP3	CASP7	BIRC2	XIAP	MMP7

possess excellent antidiabetic effect. These peptides are potentially useful in preventing or managing T2DM by targeting on various enzymes such as α -amylase, α -glucosidase and DPP-IV (Marya et al., 2018; Sharifuddin et al., 2015; Yap & Gan, 2020). The inhibition of α -amylase and α -glucosidase hinders carbohydrate breakdown and subsequent intestinal glucose absorption, whereas the inhibition of DPP-IV enhances insulin secretion and suppresses glucagon release, finally leading to the reduction of blood glucose level (Yap & Gan, 2020). The inhibition of DPP-IV represents a new strategy for T2DM treatment, and a variety of dietary proteins have been identified as a source of DPP-IV inhibitory peptides. However, the DPP-IV inhibitory effect of peptides derived from MiAMP2 and the involved mechanism of action has not yet been clarified. With the advancement of *in silico* technologies, methodologies such as molecular docking, MD simulation and network pharmacology can help improve our existing understanding of pharmacological mechanism of action of bioactive peptides derived from MiAMP2 for the treatment of diabetes.

The results of the *in silico* analysis suggested that MiAMP2 was a good source of DPP-IV inhibitory peptides, by treating with the main gastrointestinal proteases. Six peptides EQVR, EQVK, AESE, EEDNK, EECK, and EVEE were screened as potential DPP-IV inhibitory peptides. Amongst, AESE was predicted to be the most potent DPP-IV inhibitory peptide through MD simulation analysis. Numerous small peptides with DPP-IV inhibitory activities have been reported in the literature. However, the relationship between structural/compositional parameters and their DPP-IV inhibitory activity is still not quite clear. Nongonierma, Mooney, Shields, & FitzGerald (2014) found that most DPP-IV inhibitory peptides possess a hydrophobic or aromatic amino acids (Ala, Val, Ile, Leu, Met, Phe, Tyr or Trp) at their N-terminal region. Engel et al. (2003) reported that peptides interacted with the active sites of DPP-IV from their N-terminal side. Therefore, our findings suggested that the Ala at

N-terminal was crucial for the DPP-IV inhibitory ability of AESE. The active sites of DPP-IV are consisted of a hydrophobic S1 pocket and a charged S2 pocket (Engel et al., 2003; Juillerat-Jeanneret, 2014). DPP-IV inhibitory peptides were observed to form hydrophobic interactions, hydrogen bonding and van der Waals forces with catalytic residues (e.g., Tyr631, Val656, Trp659, Tyr662, Tyr666 and Val711) at hydrophobic S1 pocket, and Glu205, Glu206 or Arg125 at the S2 pocket of DPP-IV (Wang et al., 2020). Our results also showed the existence of hydrogen bonding and van der Waals forces between tetrapeptide AESE and the active sites of DPP-IV through the residues Arg125, Glu205, Glu206, Phe357, Tyr547, Ser630 and Tyr666. Additionally, it is known that DPP-IV preferentially acts on substrates bearing Pro or other small uncharged residues such as Ser and Ala at their penultimate amino acid position (Lacroix & Li-Chan, 2016), which further verified the effectiveness of AESE in the inhibition of DPP-IV.

According to the results of molecular docking and MD simulation, AESE was finally selected for network pharmacology analysis to disclose the potential signaling pathway by which it protects against diabetes. A total of 82 putative antidiabetic targets of AESE were selected by analyzing the intersection between the diabetes-associated targets and the predicted AESE targets. From the PPI network, four hub genes (BIRC2, CASP3, MMP7 and BIRC3) were identified according to the five topological algorithms (MCC, Degree, BottleNeck, Closeness, and Betweenness). Module analysis was also performed to confirm the significance of these four identified hub genes. Interestingly, two target genes CASP3 and MMP7 showed higher degrees in the cluster network. Previous studies have reported that CASP3 and MMP7 are closely related to β -cell apoptosis, renal disease and diastolic dysfunction in diabetes (Liadis et al., 2005; Zeidán-Chuliá et al., 2018). Researchers reported that high concentrations of glucose induced mitochondrial dysfunction and triggered Fas expression and β -cell apoptosis (Hodgin et al., 2013; Maedler et al., 2001). Caspase-3 (CASP3) is an essential factor for Fas-mediated cell death (Suzuki et al., 2000; Zheng et al., 1998). In our study, the regulation of CASP3 by AESE can inhibit Fas-induced apoptosis and induce β -cell proliferation. Elevated levels of matrix metalloproteinase-7 (MMP7) have been observed in serum samples of T2DM subjects (Zeidán-Chuliá et al., 2018). MMP7 (also known as matrilysin) is capable of degrading multiple extracellular matrix (ECM) proteins such as laminin, fibronectin, elastin, proteoglycans and type IV collagen. MMP-7 participates in the processing of ECM proteins during the repair and remodeling of tissues, as well as in wound healing (Malemud, 2017; Yunt et al., 2019) and is correlated with diabetic complications. Thus, alteration of MMP7 expression may represent an important mechanism for AESE mediated alleviation of diabetic complications.

The KEGG pathway enrichment results revealed that apoptosis and

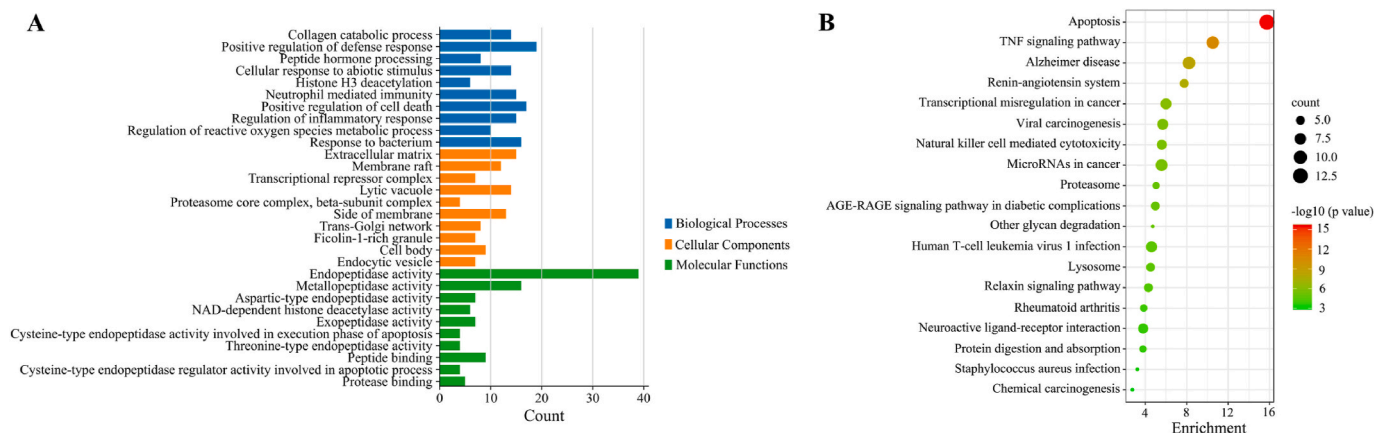


Fig. 5. Gene ontology (GO) function and Kyoto Encyclopedia of Genes and Genomes (KEGG) pathway enrichment analysis of the antidiabetic targets of AESE. (A) GO annotation; (B) KEGG pathway enrichment.

TNF signaling pathway were more enriched compared with the other classic signaling pathways. Apoptosis plays a critical role in the normal physiology of the pancreas and the pathogenesis of diabetes (Urusova, Farilla, Hui, D'Amico, & Perfetti, 2004). GLP-1 has been shown to have anti-apoptotic property (Quoyer et al., 2010) and has the ability to promote the survival of pancreatic β -cell when challenged with various apoptotic stimulators (Li et al., 2005; Yusta et al., 2006). DPP-IV inhibitory peptide AESE derived from MiAMP2 can prolong the degradation of GLP-1 by DPP-IV, thus resulting in the inhibition of β -cell apoptosis. Similarly, DPP-IV inhibitors were also demonstrated to possess anti-apoptotic activity to alleviate diabetes-associated cell/tissue damages (Liu et al., 2017; Zhang et al., 2018). The tumor necrosis factor (TNF) signaling pathway plays an important role in various physiological and pathological processes, such as cell proliferation, differentiation, apoptosis, modulation of immune responses and induction of inflammation (Vanamee & Faustman, 2018). TNF is a multi-functional proinflammatory cytokine involved in the regulation of lipid metabolism, coagulation, insulin resistance, and endothelial function (Herrmann et al., 1998; Mohallem & Aryal, 2020). A possible explanation for our observation is that AESE reduced insulin resistance and inflammatory response by lowering the expression of TNF. Six key antidiabetic targets of AESE (CASP3, CASP7, CASP8, XIAP, MMP3 and MMP9) were involved in the above two signaling pathways. Moreover, the KEGG pathway enrichment results corroborate the GO enrichment results, wherein the antidiabetic targets of AESE involved in multiple biological processes.

5. Conclusions

This study demonstrated that MiAMP2 is a good source for DPP-IV inhibitory peptides. Tetrapeptide AESE obtained from *in silico* digestion of MiAMP2 by pepsin, trypsin and chymotrypsin was supposed to be no-toxic and the most potent DPP-IV inhibitory peptide. It was found able to bind with the residues Arg125, Glu205, Glu206, Phe357, Tyr547, Ser630 and Tyr666 at the active sites of DPP-IV through hydrogen bonding and van der Waals forces. Network pharmacology-based analysis showed that AESE can interact with four hub targets BIRC2, CASP3, MMP7 and BIRC3, and ameliorate diabetes via the regulation of apoptosis and TNF signaling pathways. However, *in vivo* and *in vitro* experiments should be carried out to validate our findings in order to explore its use in functional foods for the prevention and treatment of diabetes.

CRedit authorship contribution statement

Lei Zhao: Conceptualization, Methodology, Writing – original draft, Writing – review & editing, Funding acquisition. **Mingxin Zhang:** Investigation, Visualization, Validation, Writing – original draft. **Fei Pan:** Visualization, Validation, Writing – original draft, Software, Data curation. **Jiayi Li:** Software, Data curation. **Ran Dou:** Investigation, Visualization, Validation. **Xinyi Wang:** Investigation, Visualization, Validation. **Yangyang Wang:** Investigation, Visualization, Validation. **Yumeng He:** Investigation, Visualization, Validation. **Shaoxuan Wang:** Investigation, Visualization, Validation. **Shengbao Cai:** Supervision, Funding acquisition.

Declaration of competing interest

The authors declare that they have no known competing financial interests or personal relationships that could have appeared to influence the work reported in this paper.

Acknowledgments

This work was supported by the National Natural Science Foundation of China (No. 31901698), School Level Cultivation Fund of Beijing

Technology and Business University for Distinguished and Excellent Young Scholars (BTBUY2021), Scientific Research and Entrepreneurship Plan of College Students (No. G036-2021), and the National Key Research and Development Program (Nos. 2018YFC1604203-2, 2018YFD0400403).

Appendix A. . Supplementary data

Supplementary data to this article can be found online at <https://doi.org/10.1016/j.crfs.2021.08.008>.

References

- Araki, M., Kanegawa, N., Iwata, H., Sagae, Y., Ito, K., Masuda, K., Okuno, Y., 2020. Hydrophobic interactions at subsite S1' of human dipeptidyl peptidase IV contribute significantly to the inhibitory effect of tripeptides. *Heliyon* 6 (6), e04227. <https://doi.org/10.1016/j.heliyon.2020.e04227>.
- Berendsen, H.J.C., Postma, J.P.M., van Gunsteren, W.F., DiNola, A., Haak, J.R., 1984. Molecular dynamics with coupling to an external bath. *J. Chem. Phys.* 81, 3684 <https://doi.org/10.1063/1.448118>.
- Bozbulut, R., Sanlier, N., 2019. Promising effects of β -glucans on glycaemic control in diabetes. *Trends Food Sci. Technol.* 83, 159–166. <https://doi.org/10.1016/j.tifs.2018.11.018>.
- Chen, G., Huang, K., Miao, M., Feng, B., Campanella, O.H., 2019. Molecular dynamics simulation for mechanism elucidation of food processing and safety: state of the art. *Compr. Rev. Food Sci. F.* 18 (1), 243–263. <https://doi.org/10.1111/1541-4337.12406>.
- Chen, J., Yin, B., Wang, W., Sun, H., 2020. Effects of disulfide bonds on binding of inhibitors to β -amyloid cleaving enzyme 1 decoded by multiple replica accelerated molecular dynamics simulations. *ACS Chem. Neurosci.* 11, 1811–1826. <https://doi.org/10.1021/acscchemneuro.0c00234>.
- Chin, C.H., Chen, S.H., Wu, H.H., Ho, C.W., Ko, M.T., Lin, C.Y., 2014. *cytoHubba*: identifying hub objects and sub-networks from complex interactome. *BMC Syst. Biol.* 8, S11. <https://doi.org/10.1186/1752-0509-8-S4-S11>.
- Daina, A., Michielin, O., Zoete, V., 2019. SwissTargetPrediction: updated data and new features for efficient prediction of protein targets of small molecules. *Nucleic Acids Res.* 47 (w1), W357–W364. <https://doi.org/10.1093/nar/gkz382>.
- Engel, M., Hoffmann, T., Wagner, L., Wermann, M., Heiser, U., Kiefersauer, R., Huber, R., Bode, W., Demuth, H.U., Brandstetter, H., 2003. The crystal structure of dipeptidyl peptidase IV (CD26) reveals its functional regulation and enzymatic mechanism. *PANS (Pest. Artic. News Summ.)* 100 (9), 5063–5068. <https://doi.org/10.1073/pnas.0230620100>.
- Gallego, M., Aristoy, M.C., Toldrá, F., 2014. Dipeptidyl peptidase IV inhibitory peptides generated in Spanish dry-cured ham. *Meat Sci.* 96 (2, A), 757–761. <https://doi.org/10.1016/j.meatsci.2013.09.014>.
- Gwaltney-Brant, S.M., 2013. Chapter 56 - macadamia nuts. In: Peterson, M.E., Talcott, P. A. (Eds.), *Small Animal Toxicology*, 3rd ed. Saunders, pp. 625–627. <https://doi.org/10.1016/B978-1-4557-0717-1.00056-9>.
- Han, R., Álvarez, A.J.H., Maycock, J., Murray, B.S., Boesch, C., 2021. Comparison of alcalase- and pepsin-treated oilseed protein hydrolysates – experimental validation of predicted antioxidant, antihypertensive and antidiabetic properties. *Curr. Res. Food Sci.* 4, 141–149. <https://doi.org/10.1016/j.crfs.2021.03.001>.
- Hatanaka, T., Inoue, Y., Arima, J., Kumagai, Y., Usuki, H., Kawakami, K., Kawakami, K., Mukaiyama, T., 2012. Production of dipeptidyl peptidase IV inhibitory peptides from defatted rice bran. *Food Chem.* 134 (2), 797–802. <https://doi.org/10.1016/j.foodchem.2012.02.183>.
- Herrmann, S.M., Ricard, S., Nicaud, V., Mallet, C., Arveiler, D., Evans, A., Ruidavets, J.B., Luc, G., Bara, L., Parra, H.J., Poirier, O., Cambien, F., 1998. Polymorphisms of the tumour necrosis factor-alpha gene, coronary heart disease and obesity. *Eur. J. Clin. Invest.* 28 (1), 59–66. <https://doi.org/10.1046/j.1365-2362.1998.00244.x>.
- Hodgin, J.B., Nair, V., Zhang, H., Randolph, A., Harris, R.C., Nelson, R.G., Weil, E.J., Cavalcoli, J.D., Patel, J.M., Brosius III, F.C., Kretzler, M., 2013. Identification of cross-species shared transcriptional networks of diabetic nephropathy in human and mouse glomeruli. *Diabetes* 62, 299–308. <https://doi.org/10.2337/db11-1667>.
- International Diabetes Federation, 2019. IDF Diabetes Atlas, 9th ed. International Diabetes Federation, Brussels, Belgium.
- Juilleraat-Jeanerret, L., 2014. Dipeptidyl peptidase IV and its inhibitors: therapeutics for type 2 diabetes and what else? *J. Med. Chem.* 57 (6), 2197–2212. <https://doi.org/10.1021/jm400658e>.
- Kim, B.R., Kim, H.Y., Choi, I., Kim, J.B., Jin, C.H., Han, A.R., 2018. DPP-IV inhibitory potentials of flavonoid glycosides isolated from the seeds of *Lens culinaris*: *In vitro* and molecular docking analyses. *Molecules* 23, 1998. <https://doi.org/10.3390/molecules23081998>.
- Lacroix, I.M.E., Li-Chan, E.C.Y., 2014. Isolation and characterization of peptides with dipeptidyl peptidase-IV inhibitory activity from pepsin-treated bovine whey proteins. *Peptides* 54, 39–48. <https://doi.org/10.1016/j.peptides.2014.01.002>.
- Lacroix, I.M.E., Li-Chan, E.C.Y., 2016. Food-derived dipeptidyl-peptidase IV inhibitors as a potential approach for glycaemic regulation – current knowledge and future research considerations. *Trends Food Sci. Technol.* 54, 1–16. <https://doi.org/10.1016/j.tifs.2016.05.008>.

- Lan, V.T.T., Ito, K., Ohno, M., Motoyama, T., Ito, S., Kawarasaki, Y., 2015. Analyzing a dipeptide library to identify human dipeptidyl peptidase IV inhibitor. *Food Chem.* 175, 66–73. <https://doi.org/10.1016/j.foodchem.2014.11.131>.
- Li, L., El-Kholy, W., Rhodes, C.J., Brubaker, P.L., 2005. Glucagon-like peptide-1 protects beta cells from cytokine-induced apoptosis and necrosis: role of protein kinase B. *Diabetologia* 48 (7), 1339–1349. <https://doi.org/10.1007/s00125-005-1787-2>.
- Liadis, N., Murakami, K., Eweida, M., Elford, A.R., Sheu, L., Gaisano, H.Y., Hakem, R., Ohashi, P.S., Woo, M., 2005. Caspase-3-dependent beta-cell apoptosis in the initiation of autoimmune diabetes mellitus. *Mol. Cell Biol.* 25 (9), 3620–3629. <https://doi.org/10.1128/MCB.25.9.3620-3629.2005>.
- Li-Chan, E.C., Hunag, S.L., Jao, C.L., Ho, K.P., Hsu, K.C., 2012. Peptides derived from atlantic salmon skin gelatin as dipeptidyl-peptidase IV inhibitors. *J. Agric. Food Chem.* 60 (4), 973–978. <https://doi.org/10.1021/jf204720q>.
- Lin, Z., Tong, T., Li, N., Zhu, Z., Li, J., 2020. Network pharmacology-based study of the mechanisms of action of anti-diabetic triterpenoids from *Cyclocarya paliurus*. *RSC Adv.* 10, 37168–37181. <https://doi.org/10.1039/D0RA06846B>.
- Lindorff-Larsen, K., Piana, S., Palmo, K., Maragakis, P., Klepeis, J.L., Dror, R.O., Shaw, D. E., 2010. Improved side-chain torsion potentials for the Amber ff99SB protein force field. *Proteins* 78 (8), 1950–1958. <https://doi.org/10.1002/prot.22711>.
- Liu, W., Son, D.O., Lau, H.K., Zhou, Y., Prud'homme, G.J., Jin, T., Wang, Q., 2017. Combined oral administration of GABA and DPP-4 inhibitor prevents beta cell damage and promotes beta cell regeneration in mice. *Front. Pharmacol.* 8, 362. <https://doi.org/10.3389/fphar.2017.00362>.
- Maedler, K., Spinas, G.A., Lehmann, R., Sergeev, P., Weber, M., Fontana, A., Kaiser, N., Donath, M.Y., 2001. Glucose induces beta-cell apoptosis via upregulation of the Fas receptor in human islets. *Diabetes* 50 (8), 1683–1690. <https://doi.org/10.2337/diabetes.50.8.1683>.
- Malemud, C.J., 2017. Chapter seven - matrix metalloproteinases and synovial joint pathology. In: Khalil, R.A. (Ed.), *Progress in Molecular Biology and Translational Science*, 148. Academic Press, pp. 305–325. <https://doi.org/10.1016/bbs.pmbts.2017.03.003>.
- Marya, Khan, H., Nabavi, S.M., Habtemariam, S., 2018. Anti-diabetic potential of peptides: future prospects as therapeutic agents. *Life Sci.* 193, 153–158. <https://doi.org/10.1016/j.lfs.2017.10.025>.
- Minkiewicz, P., Iwaniak, A., Darewicz, M., 2019. BIOPEP-UWM database of bioactive peptides: current opportunities. *Int. J. Mol. Sci.* 20 (23), 5978. <https://doi.org/10.3390/ijms20235978>.
- Mohalle, R., Aryal, U.K., 2020. Regulators of TNF α mediated insulin resistance elucidated by quantitative proteomics. *Sci. Rep.* 10 (1), 20878. <https://doi.org/10.1038/s41598-020-77914-1>.
- Ni, M., Hu, X., Gong, D., Zhang, G., 2020. Inhibitory mechanism of vitexin on α -glucosidase and its synergy with acarbose. *Food Hydrocolloids* 105, 105824. <https://doi.org/10.1016/j.foodhyd.2020.105824>.
- Nongonierma, A.B., Mooney, C., Shields, D.C., FitzGerald, R.J., 2014. *In silico* approaches to predict the potential of milk protein-derived peptides as dipeptidyl peptidase IV (DPP-IV) inhibitors. *Peptides* 57, 43–51. <https://doi.org/10.1016/j.peptides.2014.04.018>.
- O'Boyle, N.M., Banck, M., James, C.A., Morley, C., Vandermeersch, T., Hutchison, G.R., 2011. Open Babel: an open chemical toolbox. *J. Cheminf.* 3, 33. <https://doi.org/10.1186/1758-2946-3-33>.
- Pan, F., Li, J., Zhao, L., Tuersuntuoheti, T., Mehmood, A., Zhou, N., Hao, S., Wang, C., Guo, Y., Lin, W., 2021. A molecular docking and molecular dynamics simulation study on the interaction between cyanidin-3-O-glucoside and major proteins in milk. *J. Food Biochem.* 45 (1), e13570. <https://doi.org/10.1111/jfbc.13570>.
- Pan, F., Zhou, N., Li, J., Du, X., Zhao, L., Wang, C., Zhang, M., Ai, X., 2020. Identification of c-phycocyanin-derived peptides as angiotensin converting enzyme and dipeptidyl peptidase IV inhibitors via molecular docking and molecular dynamic simulation. *ES Food Agrofor* 2, 58–69. <https://doi.org/10.30919/esfaf1116>.
- Parrinello, M., Rahman, A., 1981. Polymorphic transitions in single crystals: a new molecular dynamics method. *J. Appl. Phys.* 52, 7182–7190. <https://doi.org/10.1063/1.328693>.
- Patel, B.D., Ghate, M.D., 2014. Recent approaches to medicinal chemistry and therapeutic potential of dipeptidyl peptidase-4 (DPP-4) inhibitors. *Eur. J. Med. Chem.* 74, 574–605. <https://doi.org/10.1016/j.ejmech.2013.12.038>.
- Pearman, N.A., Ronander, E., Smith, A.M., Morris, G.A., 2020. The identification and characterisation of novel bioactive peptides derived from porcine liver. *Curr. Res. Food Sci.* 3, 314–321. <https://doi.org/10.1016/j.crf.2020.11.002>.
- Quoyer, J., Longuet, C., Broca, C., Linck, N., Costes, S., Varin, E., Bockaert, J., Bertrand, G., Dalle, S., 2010. GLP-1 mediates antiapoptotic effect by phosphorylating Bad through a beta-arrestin 1-mediated ERK1/2 activation in pancreatic beta-cells. *J. Biol. Chem.* 285 (3), 1989–2002. <https://doi.org/10.1074/jbc.M109.067207>.
- Rost, J., Muralidharan, S., Lee, N.A., 2020. A label-free shotgun proteomics analysis of macadamia nut. *Food Res. Int.* 129, 108838. <https://doi.org/10.1016/j.foodres.2019.108838>.
- Sensory, I., 2021. A review on the food digestion in the digestive tract and the used in vitro models. *Curr. Res. Food Sci.* 4, 308–319. <https://doi.org/10.1016/j.crf.2021.04.004>.
- Sharifuddin, Y., Chin, Y.X., Lim, P.E., Phang, S.M., 2015. Potential bioactive compounds from seaweed for diabetes management. *Mar. Drugs* 13 (8), 5447–5491. <https://doi.org/10.3390/md13085447>.
- Singh, S., Sethi, S., Khanna, V., Benjamin, B., Kant, R., Patra, A.K., Rayasam, G., Mittra, S., Saini, K.S., Paliwal, J., Chugh, A., Ahmed, S., Sattigeri, J., Cliff, I., Ray, A., Bansal, V.S., Bhatnagar, P.K., Davis, J.A., 2011. RBx-0597, a potent, selective and slow-binding inhibitor of dipeptidyl peptidase-IV for the treatment of type 2 diabetes. *Eur. J. Pharmacol.* 652 (1–3), 157–163. <https://doi.org/10.1016/j.ejphar.2010.06.001>.
- Stein, S.A.M., Loccisano, A.E., Firestone, S.M., Evanseck, J.D., 2006. Principal components analysis: a review of its application on molecular dynamics data. Chapter 13 principal components analysis: a review of its application on molecular dynamics data, editor(s). David C. Spellmeyer, *Annual Reports in Computational Chemistry*. Elsevier, pp. 233–261. [https://doi.org/10.1016/S1574-1400\(06\)02013-5](https://doi.org/10.1016/S1574-1400(06)02013-5).
- Stemmer, K., Finan, B., DiMarchi, R.D., Tschöp, M.T., Müller, T.D., 2020. Insights into incretin-based therapies for treatment of diabetic dyslipidemia. *Adv. Drug Deliv. Rev.* 159, 34–53. <https://doi.org/10.1016/j.addr.2020.05.008>.
- Suzuki, A., Kawano, H., Hayashida, M., Hayasaki, Y., Tsutomi, Y., Akahane, K., 2000. Procaspase 3/p21 complex formation to resist fas-mediated cell death is initiated as a result of the phosphorylation of p21 by protein kinase A. *Cell Death Differ.* 7 (8), 721–728. <https://doi.org/10.1038/sj.cdd.4400706>.
- Trott, O., Olson, A.J., 2010. AutoDock Vina: improving the speed and accuracy of docking with a new scoring function, efficient optimization and multithreading. *J. Comput. Chem.* 31 (2), 455–461. <https://doi.org/10.1002/jcc.21334>.
- Tu, M., Cheng, S., Lu, W., Du, M., 2018. Advancement and prospects of bioinformatics analysis for studying bioactive peptides from food-derived protein: sequence, structure, and functions. *Trac. Trends Anal. Chem.* 105, 7–17. <https://doi.org/10.1016/j.trac.2018.04.005>.
- Tu, X.H., Wu, B.F., Xie, Y., Xu, S.L., Wu, Z.Y., Lv, X., Wei, F., Du, L.Q., Chen, H., 2021. A comprehensive study of raw and roasted macadamia nuts: lipid profile, physicochemical, nutritional, and sensory properties. *Food Sci. Nutr.* 9 (3), 1688–1697. <https://doi.org/10.1002/fsn3.2143>.
- Urusova, I.A., Farilla, L., Hui, H., D'Amico, E., Perfetti, R., 2004. GLP-1 inhibition of pancreatic islet cell apoptosis. *Trends Endocrinol. Metabol.* 15 (1), 27–33. <https://doi.org/10.1016/j.tem.2003.11.006>.
- Vanamee, E.S., Faustman, D.L., 2018. Structural principles of tumor necrosis factor superfamily signaling. *Sci. Signal.* 11 (511), ea04910. <https://doi.org/10.1126/scisignal.aao4910>.
- Wang, K., Yang, X., Lou, W., Zhang, X., 2020. Discovery of dipeptidyl peptidase 4 inhibitory peptides from Largemouth bass (*Micropterus salmoides*) by a comprehensive approach. *Bioorg. Chem.* 105, 104432. <https://doi.org/10.1016/j.bioorg.2020.104432>.
- Yap, P.G., Gan, C.Y., 2020. *In vivo* challenges of anti-diabetic peptide therapeutics: gastrointestinal stability, toxicity and allergenicity. *Trends Food Sci. Technol.* 105, 161–175. <https://doi.org/10.1016/j.tifs.2020.09.005>.
- Yunt, Z.X., Aschner, Y., Brown, K.K., 2019. Chapter 10 - biomarkers in IPF. In: Swigris, J. J., Brown, K.K. (Eds.), *Idiopathic Pulmonary Fibrosis*. Elsevier, pp. 99–112. <https://doi.org/10.1016/B978-0-323-54431-3.00010-X>.
- Yusta, B., Baggio, L.L., Estall, J.L., Koehler, J.A., Holland, D.P., Li, H., Pipeleers, D., Ling, Z., Drucker, D.J., 2006. GLP-1 receptor activation improves beta cell function and survival following induction of endoplasmic reticulum stress. *Cell Metabol.* 4 (5), 391–406. <https://doi.org/10.1016/j.cmet.2006.10.001>.
- Zeidan-Chulia, F., Yilmaz, D., Häkkinen, L., Könönen, E., Neves de Oliveira, B.H., Güncü, G., Uitto, V.J., Caglayan, F., Gürsoy, U.K., 2018. Matrix metalloproteinase-7 in periodontitis with type 2 diabetes mellitus. *J. Periodontol. Res.* 53 (5), 916–923. <https://doi.org/10.1111/jre.12583>.
- Zhang, D.D., Shi, N., Fang, H., Ma, L., Wu, W.P., Zhang, Y.Z., Tian, J.L., Tian, L.B., Kang, K., Chen, S., 2018. Vildagliptin, a DPP4 inhibitor, alleviates diabetes-associated cognitive deficits by decreasing the levels of apoptosis-related proteins in the rat hippocampus. *Exp. Ther. Med.* 15 (6), 5100–5106. <https://doi.org/10.3892/etm.2018.6016>.
- Zhao, W., Zhang, D., Yu, Z., Ding, L., Liu, J., 2020. Novel membrane peptidase inhibitory peptides with activity against angiotensin converting enzyme and dipeptidyl peptidase IV identified from hen eggs. *J. Funct. Foods.* 64, 103649. <https://doi.org/10.1016/j.jff.2019.103649>.
- Zheng, T.S., Schlosser, S.F., Dao, T., Hingorani, R., Crispe, I.N., Boyer, J.L., Flavell, R.A., 1998. Caspase-3 controls both cytoplasmic and nuclear events associated with Fas-mediated apoptosis *in vivo*. *PANS (Pest. Artic. News Summ.)* 95 (23), 13618–13623. <https://doi.org/10.1073/pnas.95.23.13618>.
- Zheng, J., Zheng, X., Zhao, L., Yi, J., Cai, S., 2021. Effects and interaction mechanism of soybean 7S and 11S globulins on anthocyanin stability and antioxidant activity during in vitro simulated digestion. *Curr. Res. Food Sci.* <https://doi.org/10.1016/j.crf.2021.08.003>. Available online. (Accessed 13 August 2021).
- Zhou, Y., Zhou, B., Pache, L., Chang, M., Khodabakhshi, A.H., Tanaseichuk, O., Benner, C., Chanda, S.K., 2019. Metascape provides a biologist-oriented resource for the analysis of systems-level datasets. *Nat. Commun.* 10, 1523. <https://doi.org/10.1038/s41467-019-09234-6>.